

ORIGINAL ARTICLE

Wook Kang · Chun-Won Kang · Woo Yang Chung
Chang-Deuk Eom · Hwanmyeong Yeo

The effect of openings on combined bound water and water vapor diffusion in wood

Received: December 20, 2007 / Accepted: April 18, 2008 / Published online: July 12, 2008

Abstract This study was undertaken to estimate the effect of openings between cell walls on combined bound water and water vapor diffusion in wood. Using a newly developed model, the radial and tangential moisture diffusion coefficients can be predicted depending on the opening area. The new model explicitly involves a term for water vapor diffusion through the openings, as well as a term for the combined diffusion of bound water and water vapor. A classical model developed by Stamm and Choong had higher longitudinal moisture diffusion coefficients than that in the parallel model at higher moisture content, which is inconsistent with the Wiener bound rule. The new model suggested in this article is useful for analyzing the experimental results and understanding the variability of the diffusion coefficients.

Key words Bound water · Water vapor · Conductivity · Moisture diffusivity · Wiener bound

Introduction

Moisture movement below the fiber saturation point that involves bound water and water vapor is not an advanced topic in wood physics but a classical one. The integrated theoretical approach was initiated by Stamm¹ on the assumption that the moisture movement was divided into bound

water and water vapor and that each diffusion coefficient could be estimated. Therefore, the combined bound water and water vapor diffusion depends on the ratio of the cell wall to cavity volume and the geometrical structure of the cavity. This approach can simplify the understanding of the moisture movement in wood and it is still useful to wood scientists. Choong² extended the theoretical methods to the diffusion of moisture in the longitudinal direction. In this article, the model used by Stamm¹ and Choong² is referred to as the classical model. Siau^{3,4} simplified the model by neglecting water vapor movement through the openings. The classical model and the Siau model cannot separate moisture diffusion coefficients in the radial and tangential directions.

Water vapor flows through the pit or opening simultaneously by convection and diffusion. The various models mentioned above have some limitations in this respect. Stanish et al.⁵ and Perre et al.⁶ considered the convective and diffusive water vapor movement through openings for softwood drying models. There is great difference in the effective areas of the openings between the two models; that is, 0.003–0.015 for Stanish et al.⁵ and 0.001 for Perre et al.⁶ Yeo et al.⁷ calculated the internal and external resistances for moisture movement in wood and surface evaporation from it, and experimentally determined different diffusion coefficients in each wood direction: longitudinal, radial, and tangential.

The accuracy of the simulation depends on the material parameters used. The apparent diffusivity by the experiments and the input value for simulation should have a solid physical meaning. Adapting the accurate diffusion coefficients for the simulation, however, remains a serious problem. This is largely attributed to the natural variation within and between woods. In addition, it may be responsible for the poor correlation between experiment and theory in some cases. Therefore, the objective of this study was to investigate the validity of the classical models and to develop a new model for combined bound water and water vapor diffusion. The transverse moisture diffusion coefficients for classical and Siau models are divided into radial and tangential components.

W. Kang · W.Y. Chung
Division of Forest Resources and Landscape Architecture, Chonnam National University, Gwangju 500-757, Republic of Korea

C.-W. Kang
College of Human Ecology, Chonbuk National University, Jeonju 561-756, Republic of Korea

C.-D. Eom · H. Yeo (✉)
Department of Forest Sciences, Research Institute for Agriculture and Life Sciences, Seoul National University, 599 Gwanak-ro, Gwanak-gu, Seoul 151-921, Republic of Korea
Tel. +82-2-880-4781; Fax +82-2-873-2318
e-mail: hyeo@snu.ac.kr

Modeling of combined diffusion coefficients

The mass transfer equation is expressed by Eqs. 1 and 2.

$$\frac{\partial(\rho^m m)}{\partial t} = -\nabla \cdot (\overline{j_b + j_v}) \quad (1)$$

$$\frac{\partial(\rho_c^m(1-\phi)m)}{\partial t} = -\nabla \cdot (\overline{j_b + j_v}) \quad (2)$$

where ρ^m and ρ_c^m are the wood density and cell wall density, respectively, based on oven-dry weight and moist volume (kg/m^3), m is the fractional moisture content, j_b and j_v are fluxes of bound water and water vapor ($\text{kg}/\text{m}^2\text{s}$), and ϕ is the porosity or void fraction.

The porosity of wood may be calculated from wood and cell wall density using Eq. 3, assuming that the density of bound water is equal to the water density, the oven-dry cell wall density is $1530\text{kg}/\text{m}^3$, and the pore volume remains constant with the moisture changes.⁴

$$\phi = a^2 = 1 - \frac{\rho^m}{\rho_c^m} = 1 - \frac{\rho_o}{1 + m\rho_o/1000} \frac{1 + 1.53m}{1530} \quad \forall m \leq m_{fsp} \quad (3)$$

where ρ_o is the oven-dry wood density based on oven-dry weight and oven-dry volume (kg/m^3).

It should be noted that porosity changes with moisture content. Bound water fluxes under isothermal conditions can be expressed by Fick's law:

$$j_b = -K_b \nabla m = -\rho_c^m D_B \nabla m \quad (4)$$

where K_b is the conductivity of bound water in cell wall of wood ($\text{kg}/\text{m s}$), and D_B is the diffusion coefficient of bound water in the cell wall of wood (m^2/s).

For D_B in Eq. 4, Stamm⁸ first measured it in the longitudinal direction (D_{BL}) after sealing off the lumens with molten bismuth. Siau³ converted it to the diffusion coefficient of the cell wall in the transverse direction (D_{BT}) by assuming $D_{BT} = D_{BL}/2.5$, and obtained the Arrhenius-type equation with the least-square method:

$$D_{BT} = 7 \times 10^{-6} \exp[-(38500 - 29000m)/RT] \quad (5)$$

where R is the universal gas constant ($8.314\text{J}/\text{mol K}$), and T is temperature (K). The above diffusion coefficients would not represent all wood species and some researchers use other expressions. However, the equation has been used widely in the field of wood research.⁹

For water vapor fluxes,

$$j_v = -K_v \nabla m = -\frac{D_{va}}{\tau} \frac{M_v p_{vs}}{RT} \frac{\partial h}{\partial m} \nabla m \quad (6)$$

where K_v is the conductivity of vapor in the lumen of wood ($\text{kg}/\text{m s}$), D_{va} is the bulk binary diffusivity of water vapor in air (m^2/s), τ is the tortuosity (≥ 1), h is relative humidity, M_v is the molecular weight of water vapor ($0.018\text{kg}/\text{mol}$), and p_{vs} is the saturated vapor pressure (Pa).

In Eq. 6, the bulk binary diffusivity of water vapor in air by Dushman⁴ is estimated by

$$D_{va} = 2.2 \times 10^{-5} \left(\frac{1.013 \cdot 10^5}{P} \right) \left(\frac{T}{273} \right)^{1.75} \quad (7)$$

where P is the total pressure of air and water vapor (Pa).

There is little difference in cell wall density among wood species. The diffusion coefficient of water vapor in air and saturation vapor pressure can be determined using the relevant equations. Therefore, the combined movement of bound water with water vapor could be estimated if the information on the bound water diffusion coefficient, sorption isotherm, and tortuosity are available. Tortuosity is defined as the ratio of the length of a true flow path for a fluid and the straight line distance and is always larger than 1.0.

In this study, the tortuosity effect was neglected ($\tau = 1$). Thus, water vapor diffusion coefficient of air in the lumens based on the concentration of bound water in the cell wall, D_{vc} , is calculated from

$$D_{vc} = \frac{D_{va}}{\rho_c^m} \frac{M_v p_{vs}}{RT} \frac{\partial h}{\partial m} \quad (8)$$

Neglecting the dimensional change with moisture content, the mass transfer equation, Eq. 1, can be simplified into

$$\frac{\partial m}{\partial t} = \nabla \cdot (D_b \nabla m) \quad (9)$$

The apparent directional moisture diffusion coefficients based on the concentration of bound water in wood (D_b) can be calculated by dividing conductivities (K_b) by ρ^m or $\rho_c^m(1 - \phi)$. Figure 1 shows primary paths for tangential and radial moisture transport through a cell wall (Fig. 1a) and secondary paths through a pit (Fig. 1b).

Electrical analog models for the paths have been developed. Stamm¹ proposed an electrical model to simulate the moisture transfer in the hygroscopic range shown in Fig. 2a. Figure 2b is a simplified model that integrates the secondary paths through a pit. Because the effective area of the pit openings in softwoods is small and the resistance is large, Siau⁴ neglected their effects and adopted the model shown in Fig. 2c. The contribution of the pits in hardwood is expected to be less than that in softwood because of smaller pit openings. As Siau stated, however, the effect of pit openings may be important in woods with high permeability and high specific gravity, particularly at low moisture contents and high temperature.

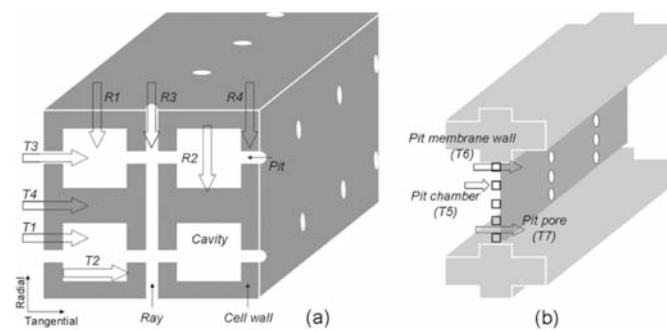


Fig. 1a, b. Primary paths for tangential and radial moisture transport through **a** a cell wall, and **b** secondary paths through a pit

For the classical model as shown in Fig. 2b, the resistance and conductance of the parallel-series model are

$$\frac{1}{R_b} = \frac{1}{R_2 + \frac{1}{\frac{1}{R_1} + \frac{1}{R_3}}} + \frac{1}{R_4} \quad (10)$$

$$g_b = \frac{1}{\frac{1}{g_2} + \frac{1}{g_1 + g_3}} + g_4 \quad (11)$$

For the Siau model of Fig. 2c, the flux direction is assumed to be perpendicular to that of the classical model.³ It should be noted that the area of cross walls and the length of side walls is different from the classical model. In this study, the geometry of cell walls used in the classical model is adopted. However, the path length through the pit for the new model is 1.0 but $1 - a$ for the classical model. Therefore, the electrical analog for the paths is somewhat different from the models.

Similarly, for the new model of Fig. 2d,

$$\frac{1}{R_b} = \frac{1}{R_1 + R_2} + \frac{1}{R_3} + \frac{1}{R_4} \quad (12)$$

$$g_b = \frac{1}{\frac{1}{g_1} + \frac{1}{g_2}} + g_3 + g_4 \quad (13)$$

Therefore, conductivity is defined by

$$K_b = g_b \frac{L_e}{A_e} \quad (14)$$

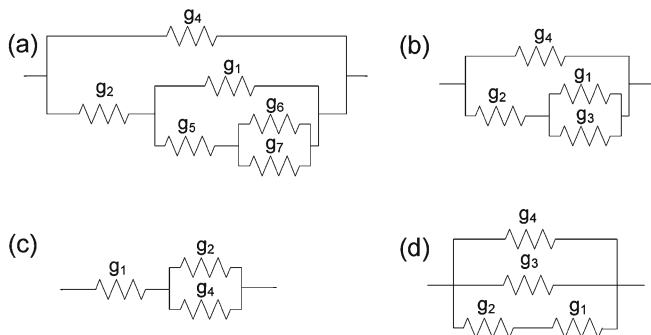


Fig. 2a-d. The electrical analog models for the paths. **a** Stamm model, **b** Stamm's simplified model, **c** Siau model, **d** new model. Conductance: g_1 , cross wall; g_2 , lumen; g_3 , pit or ray; g_4 , side wall; g_5 , pit chamber; g_6 , pit membrane wall; g_7 , pit pore

Table 1. Conductance of cell components in the principal directions

Direction	Cross walls (g_1)	Lumen (g_2)	Pit or ray (g_3)	Side walls (g_4)
Tangential	$\frac{\rho_c^m D_{BT}(a-p)}{1-a}$	$\frac{K_v(a-p)}{a}$	$K_v p \left(\frac{K_v p}{1-a} \right)^a$	$\rho_c^m D_{BT}(1-a)$
Radial	$\frac{\rho_c^m D_{BT}a}{1-a}$	K_v	$K_v r$	$\rho_c^m D_{BT}(1-a-r)$
Longitudinal	$\frac{\rho_c^m D_{BL}a(a-p)}{1-a}$	$\frac{K_v a(a-p)}{L}$	$\frac{K_v pa}{L+1-a} \left(\frac{K_v pa}{1-a} \right)^a$	$\frac{\rho_c^m D_{BL}(1-a^2)}{L+1-a}$

^aClassical model

where A_e is cross-sectional area perpendicular to flux direction and L_e is length in the flux direction.

For a mixture of solid A and void B as shown in Fig. 3, the diffusion coefficients can be derived using the mixing rules. The series model for conductance is obtained by the harmonic mean.

$$\frac{1}{g_s} = \frac{1-\phi}{g_A} + \frac{\phi}{g_B} \quad (15)$$

The parallel model is calculated using the weighted mean.

$$g_p = (1-\phi)g_A + \phi g_B \quad (16)$$

For a dispersed mixture, it may be calculated by the Maxwell model.^{10,11}

$$g_m = g_B \left(\frac{2g_B + g_A - 2(1-\phi)(g_B - g_A)}{2g_B + g_A + (1-\phi)(g_B - g_A)} \right) \quad (17)$$

The series and parallel model provide the so-called Wiener bounds,¹² which define the upper and lower bounds for the effective diffusion coefficient of a mixture. The real diffusion coefficient of any mixture should be between these boundaries. Figure 3d-f shows schematic representations of the three directional diffusion models dealt with in this study.

Results and discussion

The conductivities of wood in the principal directions can be calculated by substituting the conductivities of the cell components (Table 1) into Eqs. 11, 13, and 14. The results are as shown in Table 2.

Tangential and radial models are proposed, with a unit cube of material measured between two parallel surfaces ($A_e = 1.0$ and $L_e = 1.0$). A longitudinal model with a dimension of unit area and length of $L + 1 - a$ is proposed ($A_e = 1.0$ and $L_e = L + 1 - a$). For the classical model (the Stamm and Choong models), water vapor diffusion into the cavity and through openings is always involved in a combined term with bound water. Therefore, the classical model cannot explain the effect of water vapor through the openings in a multiphase moisture transport model.^{5,6} However, the new model explicitly involves a term for water vapor diffusion through the openings as well as the diffusion of combined bound water and water vapor.

Fig. 3a–f. Schematic representation of the diffusion models for a mixture and wood. **a** Series model, **b** parallel model, **c** dispersed mixture model, **d** tangential model, **e** radial model, **f** longitudinal model. p , Ratio of an effective pit opening area to a cross-wall or end-wall area; a , ratio of an effective diameter of lumen to diameter of cell; r , ratio of an effective ray area to a cell wall area; L , ratio of fiber length to diameter of cell

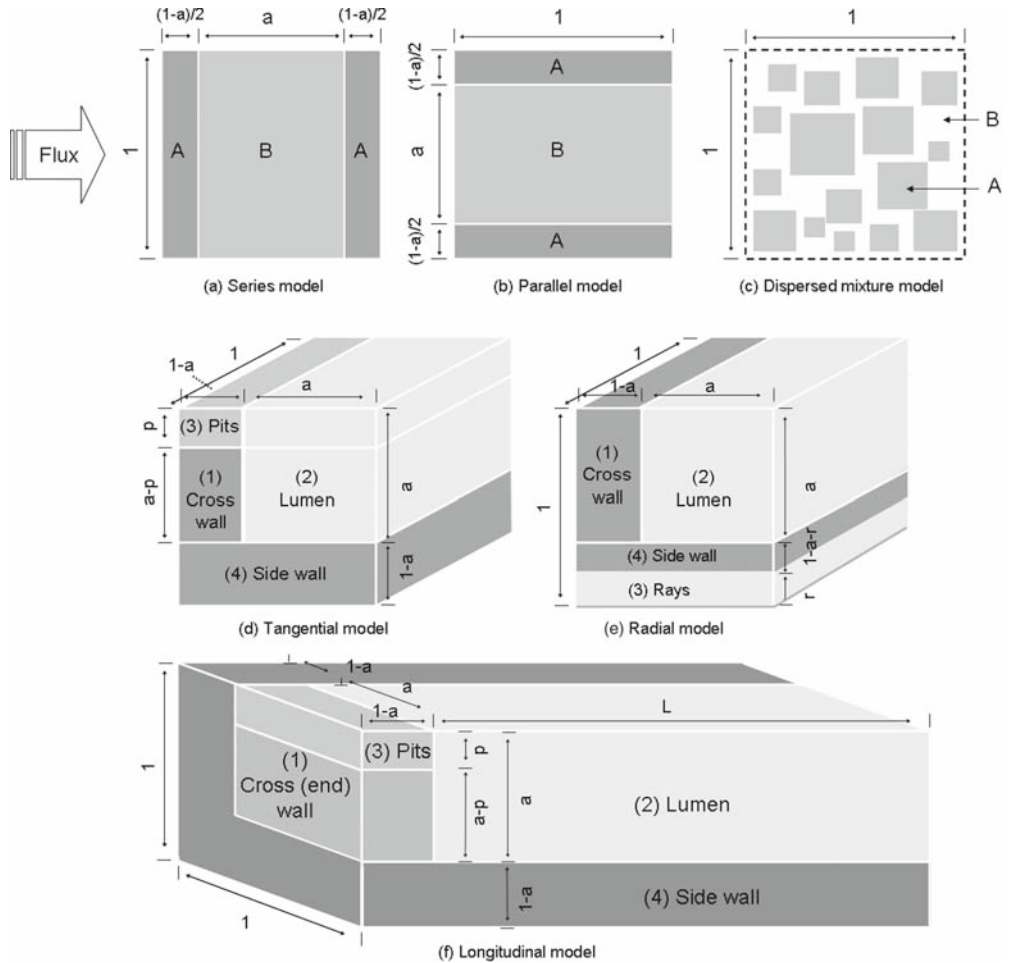


Table 2. Conductivity of wood in the principal directions

Model	Conductivities
New	
Tangential	$K_{bt} = \frac{(a-p)\rho_c^m D_{bt}}{1-a+a\rho_c^m D_{bt}/D_{vc}} + (1-a)\rho_c^m D_{bt} + pD_{vc}$
Radial	$K_{br} = \frac{a\rho_c^m D_{bt}}{1-a+a\rho_c^m D_{bt}/D_{vc}} + (1-a-r)\rho_c^m D_{bt} + rD_{vc}$
Longitudinal	$K_{bl} = \frac{a(a-p)(L+1-a)\rho_c^m D_{bl}}{1-a+L\rho_c^m D_{bl}/D_{vc}} + (1-a^2)\rho_c^m D_{bl} + paD_{vc}$
Classical	
Tangential	$K_{bt} = \frac{(a-p)[(a-p)\rho_c^m D_{bt} + pD_{vc}]}{a-p-a^2+2ap+a(a-p)\rho_c^m D_{bt}/D_{vc}} + (1-a)\rho_c^m D_{bt}$
Longitudinal	$K_{bl} = \frac{(a-p)(L+1+a)[(a-p)\rho_c^m D_{bl} + pD_{vc}]}{1-a+p(1-1/a+L/a)+L(a-p)\rho_c^m D_{bt}/D_{vc}} + (1-a^2)\rho_c^m D_{bl}$

In extreme cases where $p = a$, the diffusion model must be a parallel model because the area of the cross wall is close to zero. For the new model,

$$K_{bt} = \rho_c^m D_{bt}(1-a) + D_{vc}a \quad (18)$$

$$K_{bl} = D_{vc}a^2 + \rho_c^m D_{bl}(1-a^2) \quad (19)$$

In the classical model for $p = a$,

$$K_{bt} = \rho_c^m D_{bt}(1-a) \quad (20)$$

$$K_{bl} = \rho_c^m D_{bl}(1-a^2) \quad (21)$$

Figure 4 shows that tangential and longitudinal moisture diffusion coefficients with oven-dry specific gravity $G_0 = 0.8$ and $p = a$ at 30°C, which result from Eqs. 18–21. The new model's tangential diffusion coefficient (D_{bt}) is nearly equal to that of the parallel model, and the longitudinal diffusion coefficient (D_{bl}) is lower than that of the parallel model due to the difference in the estimated porosity.

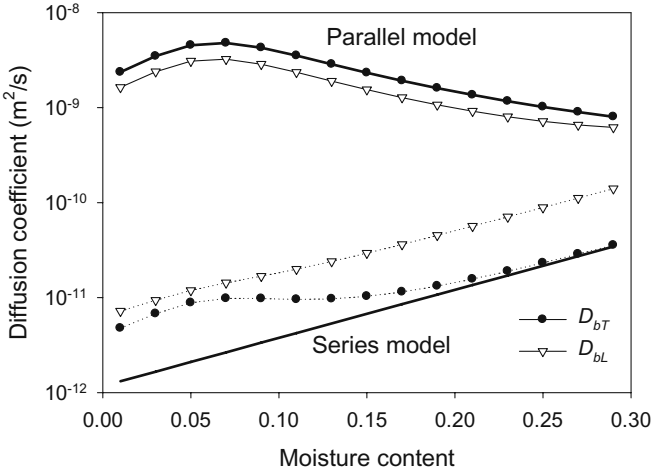


Fig. 4. Tangential and longitudinal moisture diffusion coefficients with $G_0 = 0.8$ and $p = a$ at 30°C. Solid line, new model; dotted line, classical model

However, D_{bL} and D_{bt} of the classical model are closer to those of the series model, which is erroneous and unrealistic.

The conductivities by the new model for $p = 0$ are

$$K_{bt} = \frac{a\rho_c^m D_{BT}}{1-a+\rho_c^m D_{BT}a/D_{vc}} + (1-a)\rho_c^m D_{BT} \quad (22)$$

$$= \frac{a}{1-a^2} \frac{\rho^m D_{BT}}{1-a+a\rho_c^m D_{BT}/D_{vc}} + \frac{\rho^m D_{BT}}{1+a}$$

$$K_{bL} = \frac{a^2}{1-a^2} \frac{(L+1-a)\rho^m D_{BL}}{1-a+L\rho_c^m D_{BL}/D_{vc}} + \rho^m D_{BL} \quad (23)$$

For the classical model for $p = 0$, the conductivities are

$$K_{bt} = \frac{a}{1-a^2} \frac{\rho^m D_{BT}}{1-a+a\rho_c^m D_{BT}/D_{vc}} + \frac{\rho^m D_{BT}}{1+a} \quad (24)$$

$$K_{bL} = \frac{a^2}{1-a^2} \frac{(L+1-a)\rho^m D_{BL}}{1-a+L\rho_c^m D_{BL}/D_{vc}} + \rho^m D_{BL} \quad (25)$$

The tangential conductivity of the classical model is the same as that of the new model, but the longitudinal conductivity is slightly different between the classical and new models.

Figure 5 shows D_{bt} and D_{bL} for $p = 0$. There is little difference between the Siau model and the new model in terms of D_{bL} . The D_{bL} in the classical model is always higher than that in the new model and the Siau model. The classical model has a higher D_{bL} than that in the parallel model at higher moisture content, which is inconsistent with the Wiener bound rule. The D_{bt} or transverse moisture diffusion coefficients in the Siau model are always $1/a$ times higher than those in the new model because of the larger area of the cross walls and the smaller area of the side walls. As the wood density increases, therefore, the difference between the Siau model and the new model increases.

Figures 6 and 7 show the moisture diffusion coefficients at various p , respectively, for $G_0 = 0.4$ $G_0 = 0.8$. The effect of the openings is more important in woods with higher

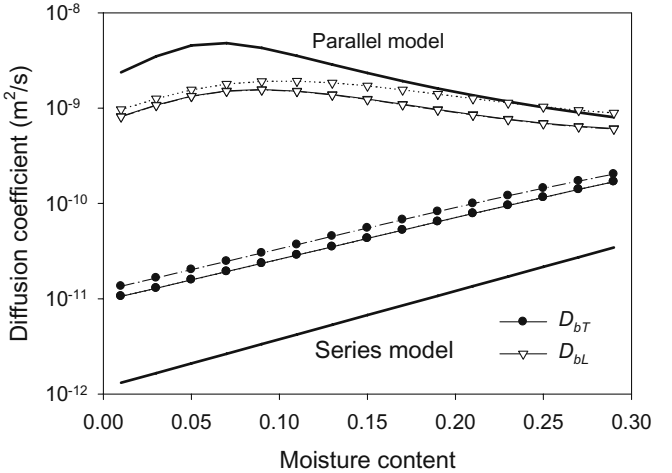


Fig. 5. Tangential and longitudinal moisture diffusion coefficients with $G_0 = 0.8$ and $p = a$ at 30°C. Solid line, new model; dotted line, classical model; dash dotted line, Siau model

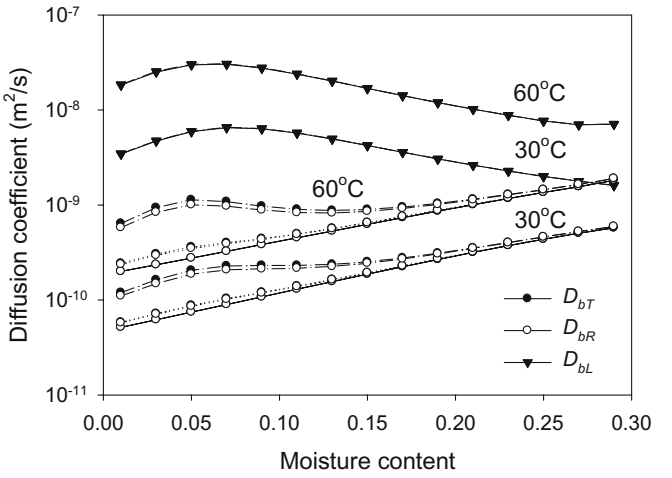


Fig. 6. Moisture diffusion coefficients with $G_0 = 0.4$ at various p . Solid line, p (or r) = 0; dotted line, p (or r) = 0.001; dash dotted line, p (or r) = 0.01

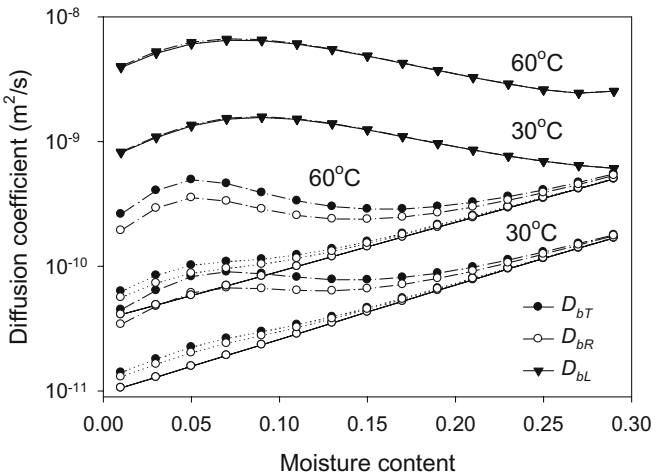


Fig. 7. Moisture diffusion coefficients with $G_0 = 0.8$ at various p . Solid line, p (or r) = 0; dotted line, p (or r) = 0.001; dash dotted line, p (or r) = 0.01

permeability and higher specific gravity, particularly at lower moisture contents and higher temperature. For woods with higher permeability, D_{bt} and D_{br} are nearly constant with moisture content. Depending on the magnitude of p and r , the ratio of radial and tangential diffusion coefficients may change. Because the tangential model and the radial model have the same schematics when p and $r = 0$, the marks of D_{bt} and D_{br} in the figures overlap each other.

Conclusions

The flux and path length of water vapor were corrected in terms of the combined bound water and water vapor diffusion coefficients that were originally deduced by Stamm.¹ The transverse moisture diffusion coefficients in the Siau model were always higher than those in the new model by a factor equivalent to the inverse of the ratio of effective diameter of the lumen to the diameter of the cell, because of the larger area of the cross walls and the smaller area of the side walls. The new model can predict radial and tangential diffusion coefficients. The new model explicitly involves a term for water vapor diffusion through the openings as well as combined diffusion of bound water with water vapor. It may be helpful for analyzing the experimental results of the diffusion coefficients and understanding the variability. In addition, it would be useful for calculating the effect of moisture flux on heat transfer. For woods with larger openings or higher permeability, the apparent diffusion coefficient might be near constant with changing moisture content.

Acknowledgments This work was supported by a Korea Research Foundation Grant funded by the Korean Government (MOEHRD) (Regional Research Universities Program/Biohousing Research Institute) and carried out with the support of “Forest Science and Technology Projects” provided by Korea Forest Service.

References

1. Stamm AJ (1960) Combined bound-water and water vapour diffusion into Sitka spruce. *Forest Prod J* 10:644–648
2. Choong ET (1965) Diffusion coefficients of softwoods by steady-state and theoretical methods. *Forest Prod J* 15:21–27
3. Siau JF (1984) Transport processes in wood. Springer, Berlin Heidelberg New York
4. Siau JF (1995) Wood: influence of moisture on physical properties. Virginia Polytechnic Institute and State University
5. Stanish MA, Schajer GS, Kayhan F (1986) A mathematical model of drying for hygroscopic porous media. *AIChE J* 32:1301–1311
6. Perre P, Moser M, Martin M (1993) Advances in transport phenomena during convective drying with superheated steam and moist air. *Int J Heat Mass Transfer* 36:2725–2746
7. Yeo H, Smith WB, Hanna RB (2002) Mass transfer in wood evaluated with a colorimetric technique and numerical analysis. *Wood Fiber Sci* 34:657–665
8. Stamm AJ (1959) Bound-water diffusion into wood in the fiber direction. *Forest Prod J* 9:27–32
9. Kang W, Chung WY, Eom CD, Yeo H (2008) Some considerations in heterogeneous nonisothermal transport models for wood: a numerical study. *J Wood Sci*. doi: 10.1007/s10086-007-0938-0
10. Maxwell JC (1904) A treatise on elasticity and magnetism, 3rd edn. Clarendon, Oxford, UK
11. Wang J, Carson JK, North MF, Cleland DJ (2006) A new approach to modelling the effective thermal conductivity of heterogeneous materials. *Int J Heat Mass Transfer* 49:3075–3083
12. Wiener O (1912) Der Abhandlungen der Mathematisch-Physischen Klasse der Königl. Sächsischen Gesellschaft der Wissenschaften 32:509–604